The membrane activity of BOK involves formation of large, stable toroidal pores and is promoted by cBID

Yuniel Fernández-Marrero[1], Stephanie Bleicken[2,3], Kushal Kumar Das[2], Daniel Bachmann[1], Thomas Kaufmann[1, *] and Ana J Garcia-Saez[2, *].

[1]Institute of Pharmacology, University of Bern, Bern, Switzerland

[2]Interfaculty Institute of Biochemistry, University of Tübingen, Tübingen, Germany

[3]Current address: Zentrum für molekulare Spektroskopie und Simulation solvensgesteuerter Prozesse, Ruhr-Universität Bochum; Bochum, Germany.

*Both authors contributed equally to this work.

Article type : Regular Paper

To whom correspondence should be addressed:

Ana García-Sáez, PhD
Interfaculty Institute of Biochemistry
University of Tübingen
72076 Tübingen
Germany
Phone: +49-7071-29-73318
Fax: +49-7071-29-5070
e-mail: ana.garcia@uni-tuebingen.de

Thomas Kaufmann, PhD
Institute of Pharmacology
University of Bern
Inselspital, INO-F
CH-3010 Bern, Switzerland
Phone: +41-31-632-32-89
Fax: +41-31-632-49-92
e-mail: thomas.kaufmann@pki.unibe.ch

Running title: BOK forms stable pores in membranes

Keywords: BOK, apoptosis, pore, permeabilisation, BCL-2 family, membrane, liposome, mitochondria

Conflict of interest: the authors declare no conflict of interests.

Abbreviations: **LUV**, large unilamellar vesicles; **GUV**, giant unilamellar vesicles; **CL**, cardiolipin; **PC**, phosphatidylcholine; **PE**, phosphatidylethanolamine; **PI**, L-α-phosphatidylinositol; **PS**, phosphatidylserine; **PA**, phosphatidic acid; **LPC**, lysophosphatidylcholine; **Chol**, cholesterol; **PG**, phosphatidylglycerol; **Sph**, sphingomyelin; **DiI**, 1,1'-dioctadecyl-3,3,3',3-tetramethylindocarbocyanine perclorate; **cyt. c**, cytochrome c; **APC**, allophycocyanin, **AF488**, AlexaFluor-488 dye; **DPBS**, Dulbecco's Phosphate-Buffered Saline; **MEF**, murine embryonic fibroblast; **ER**, endoplasmic reticulum.

ABSTRACT

The BCL-2 family members are key regulators of the intrinsic apoptotic pathway, which is defined by permeabilisation of the mitochondrial outer membrane by members of the BAX-like subfamily. BOK is classified as a BAX-like protein; however, its (patho-)physiological role remains largely unclear. We therefore assessed the membrane permeabilisation potential of C-terminally truncated recombinant BOK, $BOK^{\Delta C}$. We show that $BOK^{\Delta C}$ can permeabilize liposomes mimicking the composition of mitochondrial outer membrane, but not of endoplasmic reticulum, forming large and stable pores over time. Importantly, pore formation was enhanced by the presence of cBID and refractory to the addition of anti-apoptotic BCL-X_L. However, isolated mitochondria from *Bax*$^{-/-}$*Bak*$^{-/-}$ cells were resistant to BOK-induced cytochrome c release, even in presence of cBID. Taken together, we show that $BOK^{\Delta C}$ can permeabilize liposomes, and cooperate with cBID, but its role in directly mediating mitochondrial permeabilisation is unclear and may underlie a yet to be determined negative regulation.

INTRODUCTION

The members of the BCL-2 family are critical regulators of the intrinsic apoptotic pathway, which is defined by mitochondrial outer membrane permeabilisation (MOMP). The members of the family contain up to four short conserved BCL-2 homology domains (BH1-4) and are subdivided into the pro-apoptotic BH3-only proteins or the multi-BH domain members. The latter comprises the prosurvival BCL-2-like group (BCL-2, MCL-1, BCL-X_L and BFL-1/A1) and the pro-apoptotic BAX-like group (BAX, BAK and maybe BOK) [1].

Currently, it is accepted that in the absence of cellular stress these proteins co-exist in a network of balanced interactions, neutralizing each other in their functions. Upon metabolic, pathogen- or damage-induced cellular stress, the network is altered resulting in apoptotic cell death or survival, depending on the magnitude of the insult. During apoptosis, MOMP is promoted by the oligomerization of BAX and/or BAK resulting in the release to the cytosol of apoptogenic proteins from the mitochondrial intermembrane, including cytochrome c and SMAC/DIABLO, with subsequent activation of caspases [2]. A pre-requisite for MOMP is the disengagement of BAK from anti-apoptotic MCL-1 and BCL-X_L, as well as recruitment of cytosolic BAX to the MOM [3]. A well-known factor aiding BAX translocation and mitochondrial pore formation is the p15 fragment of the BH3-only protein BID [4]. BID is proposed to interact transiently with BAX, promoting the conformational changes for BAX membrane insertion in a catalyst-like manner [4]. Importantly, the lipid composition of the membranes where these proteins exert their activities provide an extra layer of complexity [5, 6]. Cardiolipin, a mitochondria-specific phospholipid, seems crucial for the concerted activity of cBID and BAX [7-10].

BCL-2-related ovarian killer (BOK, gene name *BOK* or *BCL2L9*) is a 23.4 kDa protein highly conserved in the animal kingdom, with sequence homology to BAK and BAX [11]. In contrast to BAX or BAK, BOK predominantly localizes to the membranes of the endoplasmic reticulum (ER) and the Golgi apparatus, and to a lesser extent to mitochondria [12]. BOK is widely expressed and readily detectable at protein level in mouse tissues, with high expression in reproductive tissues, brain, kidney, spleen and gastrointestinal tract [12, 13]. BOK function in cells is enigmatic. Although enforced expression of BOK induces apoptosis [11, 12, 14, 15], genomic deletion of *Bok/Bak* or *Bok/Bax* did not produce an enhanced phenotype beyond that accounted for *Bax* or *Bak* single knockout mice, with the exception of increased oocyte numbers in $Bok^{-/-}Bax^{-/-}$ females [16]. Recent work from Ke *et al.* on a chimeric mouse with a $Bok^{-/-}Bak^{-/-}Bax^{-/-}$ triple knockout hematopoietic system provided evidence that BOK's redundancy with BAX and BAK exists but might be restricted to specific tissues [17]. However, other studies suggest that depending on the tissue or the nature of the apoptotic stressor, BOK may have non-apoptotic functions, such as in trophoblast proliferation [18], or may even have a pro-survival function [12, 19].

BOK has been shown to interact with IP3 receptors, protecting IP3Rs from caspase-mediated degradation and BOK from proteasomal degradation [20, 21]. Degradation of BOK via the ubiquitin/proteasome was also shown by Llambi et al. in the context of the ERAD pathway [14]. This paper also describes a BAX-like apoptosis inducing function of BOK when the ERAD pathway is blocked [14].

In this work, we generated an untagged, C-terminally truncated version of recombinant BOK ($BOK^{\Delta C)}$, and characterized its pore forming potential in liposomes and isolated mitochondria. $BOK^{\Delta C}$ provoked the permeabilisation of artificial membranes by forming long-lived toroidal pores, large enough for passage of a 104 kDa protein. $BOK^{\Delta C}$'s induced pore formation strongly depended on the lipid composition, with liposomes resembling MOM being much more efficiently permeabilized than those mimicking ER composition. Importantly, we provide solid evidence that cleaved BID (cBID) cooperates with $BOK^{\Delta C}$ in pore formation, while BCL-X_L was unable to inhibit $BOK^{\Delta C}$ activity. Strikingly, however, our studies on mitochondria isolated from $Bax^{-/-}Bak^{-/-}$ cells indicated that $BOK^{\Delta C}$ is highly inefficient in promoting MOMP, even in the presence of cBID or after heat activation. Overall, these data indicate that despite its effects on artificial membranes, the role of BOK on biological membranes may be subject to yet to be described negative regulatory mechanisms.

RESULTS

Purification of recombinant BOK$^{\Delta C}$

BCL-2 proteins have been purified in the past by affinity-based methodologies using histidine or GST tag-based approaches. Tagged proteins come with the risk of introducing artifacts. One notable exception is the purification of full length BAX and BCL-X_L in bacteria using an intein-chitin binding domain fused to their C-terminus [22, 23]. The intein domain can be subsequently removed by addition of dithiothreitol, releasing the untagged protein with a high purity degree in one step. Based on these advantages we decided to use the same approach to produce recombinant BOK and its C-terminally truncated form, BOK$^{\Delta C}$. A major pitfall while establishing the purification workflow was the amount of contaminants present in the elution from the chitin-affinity step. One explanation would lie in the acidic nature of the *E. coli* proteome [24, 25] contrasting with the high isoelectric point (pI) of BOK, which seems unique amongst the multidomain members of the BCL-2 family (Figure 1A), thus favoring the binding of unwanted proteins. To overcome this effect, we incorporated a cation exchange step while working at high salt concentration and pH. This method has been reported to outperform those using Ni-NTA and GST for the purification of basic proteins [26]. The purified full length BOK did not reach an acceptable purity and the total yield was extremely low, likely due to protein aggregation because of its hydrophobic C-terminal tail. On the other hand, significantly higher amounts (300-700 µg protein from 5 L culture) of pure (>90%) BOK$^{\Delta C}$ could be purified, which is comparable to the purification of BAX (Figure 1B-D). Therefore, we decided to work with BOK$^{\Delta C}$. The identity of the purified protein was assessed using western blotting and mass spectrometry (Figure 1C and data not shown).

BOK$^{\Delta C}$ induces membrane permeabilisation of large unilamellar vesicles depending on the lipid composition

We hypothesized that BOK follows a similar mechanism of action as BAX and BAK when interacting with membranes. Thus, we explored the potential of recombinant BOK$^{\Delta C}$ to promote membrane permeabilisation, by following content release of the fluorophore calcein (~1 kDa) from large unilamellar vesicles (LUVs). Since BOK, under physiological conditions, is largely localized to the membranes of the ER [12], we reasoned that BOK might differentially affect artificial membranes mimicking ER or MOM lipid composition. Indeed, LUVs made from a mitochondria-like lipid mixture (MITOmix) were readily permeabilized, in contrast to those resembling an ER lipid composition (ERmix), which required much higher protein concentrations to reach comparable permeabilisation levels (Figure 2A).

A major difference in those membrane model compositions was the presence of the mitochondria-specific lipid cardiolipin in MITOmix while it was absent from ERmix. Hence, we decided to test the contribution of this lipid to the $BOK^{\Delta C}$ -induced calcein release. As shown in Figure 2B, the CL content positively correlated with $BOK^{\Delta C}$ -induced calcein release from LUVs.

Cardiolipin is a negatively charged phospholipid inducing intrinsic monolayer curvature that has been suggested to play a specific role in BAX pore formation [8]. To find out whether this is also the case for $BOK^{\Delta C}$, or whether it is a general charge effect, we substituted CL for phosphatidylglycerol (PG) (Figure 2B). When a similar proportion of PG was used in the assay, the dye release was similar, suggesting that the overall negative charge of the membrane plays a role in the pore activity of $BOK^{\Delta C}$.

The pores formed by $BOK^{\Delta C}$ show features of toroidal pores

Several lines of evidence suggest that BAX and BAK form toroidal pores, which involve the participation of lipids at the pore edge. Consequently, these pores would be affected by lipids modulating the intrinsic membrane curvature. The formation of non-lamellar structures, like toroidal pores, frequently requires the presence of lipids with opposite geometrical and intrinsic curvature properties to compensate the defective packaging in the pore rim [27]. To investigate the impact of the lipid geometry on $BOK^{\Delta C}$ -induced membrane permeabilisation, we varied the concentrations of CL (cone, negative curvature inducer) and lysophospatidylcholine (LPC) (inverted cone, positive curvature inducer). Surprisingly, even small amounts of LPC enabled $BOK^{\Delta C}$ -mediated calcein release to a degree comparable to that obtained using 20% of CL (Figure 2C). This effect was further enhanced when CL and LPC were combined in the same vesicles, in line with the idea that $BOK^{\Delta C}$ could be involved in the formation of non-lamellar structures like toroidal pores. However, we could not discard the possibility that the role of CL was merely due to its negative curvature. To corroborate this, we included phosphatidic acid (PA) in our analysis, which is a lipid that combines negative charge and a very pronounced negative curvature. Indeed, from all the binary lipid mixtures tested, those containing PA exhibited the highest sensitivity to $BOK^{\Delta C}$ treatment (Figure 2D). Additionally, we also used cholesterol, which is a neutral lipid with a high negative curvature; indeed, addition of cholesterol also increased $BOK^{\Delta C}$ mediated dye release, although its impact was lower than that of LPC (Figure 2D). These results demonstrate that $BOK^{\Delta C}$ membrane activity largely depends on the presence of negatively charged lipids and on their intrinsic curvature, suggesting that $BOK^{\Delta C}$ pores are of toroidal nature.

cBID cooperates with BOK$^{\Delta C}$ to form pores that allow the passage of the 104 kDa protein APC

Considering the concerted mechanism described for cBID to activate BAX to form pores in membranes [28], we tested if the membrane activity of BOK$^{\Delta C}$ would be modulated by cBID in a similar manner. Since BOK$^{\Delta C}$ could permeabilize LUVs of several lipid compositions, we choose the MITOmix for these experiments due to its physiological relevance and positive, but still moderate, reactivity to BOK$^{\Delta C}$.

We first determined the BOK$^{\Delta C}$ concentration that *per se* induced 50% of the maximum calcein release in the LUVs (7 nM, Figure 3A), which was then used together with serial dilutions of cBID to test for synergy. Surprisingly, cBID**,** but not its BH3 peptide nor a BIM BH3 peptide, clearly exacerbated the calcein release activity of BOK$^{\Delta C}$ (Figure 3B**,** C). Of note, cBID also clearly enhanced the calcein release activity of full length BOK (Figure 3B).

At this point, we hypothesized that, similar to BAX, BOK$^{\Delta C}$ could promote the trespassing of molecules bigger than calcein (>1 kDa). To investigate the dimension of BOK$^{\Delta C}$ -mediated membrane pores, we used cell-sized vesicles known as giant unilamellar vesicles (GUV), composed of the MITOmix and a lipid dye to visualize the membrane. We incubated GUVs with two differently sized proteins: AlexaFluor-488 conjugated cytochrome c (cyt. $c_{488;}$ 12 kDa) and allophycocyanin (APC; 104 kDa) and followed their passage through the membrane in presence or absence of cBID, or cBID plus BCL-X_L. As positive and negative references we used cBID and BAX in presence or absence of BCL-X_L after incubation time of 60 minutes, as shown before [29, 30].

Using the previous conditions in this membrane model, BOK$^{\Delta C}$ alone had negligible activity at 10 nM concentration, but the population of non-permeabilized GUVs was significantly reduced in the samples treated with BOK$^{\Delta C}$ and cBID. This effect was comparable to the positive control, BAX plus cBID (Figure 3D) and confirmed the cBID effect on BOK activity observed in the calcein assay. Interestingly, and contrasting with cBID/BAX, the permeabilisation of GUVs by cBID/BOK$^{\Delta C}$ was not inhibited by BCL-X_L. Analysis of individual vesicles revealed that most were simultaneously filled with both dyes, indicating that the pores formed by BOK$^{\Delta C}$ plus cBID are permissive to molecules up to the size of 104 kDa (APC) (Figure 3E).

BOK$^{\Delta C}$-induced membrane permeabilisation can be accomplished by thermal activation

A simplistic but still efficient approach described by Pagliari *et al*. used thermal activation of BAX and BAK to promote cyt. c release from isolated mitochondria [31]. A similar strategy has also been used to induce BAX oligomerization and pore formation on GUVs [29] and LUVs [32]. After the robust permeabilisation induced by BOK$^{\Delta C}$ alone, we investigated the energetic threshold of this effect.

We co-incubated BOK$^{\Delta C}$ or BAX with MITOmix-derived GUVs for 45 min at 42°C and evaluated the permeabilisation to cyt. c_{488} and APC. As shown in Figure 4A, heat activated BOK (as well as BAX) facilitated the passage of both permeabilisation tracers into GUVs, indicating that cBID is not necessary for BOK$^{\Delta C}$ to form pores capable of accommodating a wide range of molecular sizes (Figures 4A, B) and that also in this aspect BOK activity is similar to BAX.

BOK$^{\Delta C}$ forms long-lived pores

After establishing the GUV permeabilisation potential by BOK$^{\Delta C}$, we tested if BOK$^{\Delta C}$ pores were transient and unstable structures or if they remained stably open under equilibrium conditions. To address this question, we used an assay previously described [30, 33] in which two additional dyes of different size are added to GUVs preincubated with BCL-2 proteins that have induced pores. If the dyes are still able to enter the vesicles, this indicates that the membrane permeabilized state is stable at least during the incubation time.

We incubated MITOmix-derived GUVs for 45 minutes with BOK$^{\Delta C}$ plus cBID in the presence of free AlexaFluor-555 (AF555) dye. Immediately after that we added cyt. c_{488} and APC to the wells and determined their incorporation into the vesicles within 15 min. This narrow time window guaranteed that vesicles filled with these proteins were most likely due to the existence of a pre-formed pore rather than to newly formed ones. Finally, the sample was imaged in order to detect whether cyt. c_{488} and APC could also trespass the membrane through the formed pores (Figure 5A), which would be indicative of cBID/BOK$^{\Delta C}$ creating long-lived pores. Moreover, this experiment provides information about the pore size under equilibrium conditions and tests the impact of BOK$^{\Delta C}$ concentration on the pore size.

The distribution of AF555 incorporation into GUVs was quantified (Figure 5B). As expected from the experiments shown above, GUV permeabilisation positively correlated with the amount of BOK$^{\Delta C}$ used. Interestingly, we noticed a decrease of GUVs per area, proportional to the concentration of BOK$^{\Delta C}$ (Figure 5C). We attribute this to the membrane destabilizing impact of the pore formation process, which, combined with the mechanical stress provided while adding the size markers, contribute to GUV destruction. A less pronounced, but still similar effect has been reported for BAX [30]. Afterwards, we focused on GUVs already filled with AF555, which indeed consistently incorporated cyt. c_{488} and APC. These results indicate that the initial pores remained permissive and stable during the time of the assay (Figures 5D, E).

BOK$^{\Delta C}$ is inefficient in releasing cyt. c from isolated mitochondria

Since the membrane activity of BOK$^{\Delta C}$ was comparable to that of BAX, we next wanted to determine whether the BOK$^{\Delta C}$ pore-forming activity demonstrated *in vitro* had biological implications in the context of mitochondria. We explored if recombinant BOK$^{\Delta C}$ could mediate cyt. c release from mitochondria isolated from *Bax*$^{-/-}$*Bak*$^{-/-}$ double deficient mouse embryo fibroblasts (MEF). Of note, and contrary to our findings in artificial lipid vesicles, BOK$^{\Delta C}$ was unable to permeabilize mitochondria, even in the presence of cBID (Figure 6A). Furthermore, we incubated *Bax*$^{-/-}$*Bak*$^{-/-}$ mitochondria with BOK$^{\Delta C}$ at 43°C to recapitulate the heat activation process [31]. Surprisingly, and in contrast to BAX, BOK$^{\Delta C}$ was again unable to promote MOMP in those mitochondria (Figure 6B). Strikingly, this lack of activity in mitochondria is not the result of impaired interaction with the membrane, since we clearly detected association of BOK$^{\Delta C}$ with crude mitochondrial membranes isolated from *Bok*$^{-/-}$ cells (Figure 6C). This was also corroborated by sucrose gradient fractionation after co-incubation of BOK$^{\Delta C}$ with crude BOK-deficient mitochondrial fractions. In this case BOK$^{\Delta C}$ adopted a uniform distribution gradient not restricted to the mitochondria containing fractions, irrespective of the addition of cBID (Figure 6 D).

DISCUSSION

BOK remains an enigmatic and controversial protein among the BCL-2 members. In accordance with its sequence homology with BAX/BAK, multiple studies, including our own work, demonstrated that BOK promotes intrinsic apoptosis upon overexpression [11, 12, 14, 34]. However, both BAX/BAK-dependent as well as BAX/BAK-independent mechanisms have been proposed since [12, 14, 34]. Currently, there is limited evidence for a pro-apoptotic role for BOK under physiological and pathophysiological conditions, and several studies even point towards protective roles of BOK in certain tissues or in response to specific stressors [12, 13, 16-19, 34-36].

We describe an approach to purify recombinant BOK from bacteria, combining affinity and ion exchange-based techniques. In our exploratory experiments, we used full length BOK, and detected comparable pore activity to the truncated protein (data not shown). However, we could not exclude that the insertion of the transmembrane region simply following thermodynamic principles was responsible for this effect. Thus, we decided to use an untagged, truncated version lacking the last 24 amino acids (BOK$^{\Delta C24}$, [12]), which resulted also in higher yields and purity.

Interestingly, BOK seems to predominantly localize to the membranes of the ER, where it interacts with IP3 receptors, and where it is subject to ubiquitylation and proteasomal turnover [12, 14, 20, 21]. In spite of this, addressing the question whether BOK can permeabilize the mitochondrial outer membrane and induce MOMP in a manner similar to BAX/BAK seems absolutely critical to better understand the role and function of BOK. In a recent study, Llambi and colleagues have provided evidence that recombinant BOK (more precisely an 8xHis-tagged, C-terminally truncated version) can

have pore-forming activity in liposomes, which, intriguingly, does not seem to require cooperation with activator BH3-only proteins (e.g. tBID) [14]. However, the ability to permeabilize membranes has also been reported for other BCL-2 proteins, like BCL-X_L, BCL-2 or cBID, with lack of correlation regarding a direct function in MOMP and therefore caution is advised with the interpretation of simple experiments of liposome permeabilisation.

In this work, we analyzed in detail the pore forming potential of recombinant $BOK^{\Delta C}$ in artificial liposomes and isolated mitochondria. We confirmed the recently described ability of $BOK^{\Delta C}$ to permeabilize artificial membranes on its own [14] and demonstrate that the main features of BOK pore activity resemble those of BAX and BAK. The lipid composition of biomembranes strongly defines critical physicochemical properties like overall charge, intrinsic curvature and fluidity. A concerted interplay of these parameters with membrane proteins guarantees important physiological processes e.g. membrane fission and fusion, organelle shape or protein-lipid segregation in microdomains [37]. Our data from calcein assays indicated that $BOK^{\Delta C}$ permeabilized vesicles in function of their overall negative charge and greatly depending on the intrinsic curvature of those membranes. This link on lipid composition and activity of BCL-2 proteins has been documented as a key determinant of BAX, BAK, BIM and BID activities [5, 9, 10].

Further evaluation of $BOK^{\Delta C}$ -mediated pores in GUVs indicated that they have sufficient size to allow the passage of large proteins like cyt. c and APC, and that those pores remain stable over time, resembling those described for BAX [23]. This, together with the large dependence on lipid geometry, strongly suggests that the membrane pores induced by BOK are toroidal. As with BAX, our data support the participation of lipids in the pore structure as well as the formation of flexible, undefined pores that reach large sizes and remain open for a long time. Additional studies will be required to elucidate if BOK pores are also tunable in size [30] and correlate with a mixture of BOK oligomeric species [32], as well as if arc- and/or ring-like assemblies of BOK line the pore walls [38]. Importantly, however, and in contrast to BAX plus cBID, BOK or BOK plus cBID induced pores independently of the presence of BCL-X_L.

Of note, we demonstrate here that cBID, but not its derived BH3-peptide, cooperates with $BOK^{\Delta C}$ to induce permeabilisation of artificial membranes modeling the mitochondrial lipid composition. This cooperation was noticeable beyond the point of equimolarity between the proteins, suggesting that cBID is less efficient in promoting BOK activity than in activating BAX. This result contrasts with the data provided by Llambi et al [14] who concluded that BOK is constitutively active, independently of the influence of activator BH3-only proteins, or any other BCL-2 protein. Whereas we used untagged $BOK^{\Delta C}$, Llambi et al. used an 8xHis-tagged $BOK^{\Delta C}$, which was then artificially aggregated using Ni-NTA. It is conceivable to speculate that Ni-NTA may very strongly activate

BOK, thereby masking a possible cooperative effect by BH3-only peptides. Importantly, we further provide evidence that cBID also cooperates with full length BOK.

We also report that the pore activity of cBID/ $BOK^{\Delta C}$ is not inhibited by BCL-X_L. This is unexpected, as based on the literature, BCL-X_L should sequester cBID, thereby preventing the activation of $BOK^{\Delta C}$. We speculate that the interaction between cBID and $BOK^{\Delta C}$ induces conformational changes hindering the interaction between cBID and BCL-X_L. A direct inhibition of $BOK^{\Delta C}$ by BCL-X_L on the other hand seems unlikely, as others and we have failed to show interaction between these two proteins [11, 12, 39]. Considering the "helix-loop-helix" secondary structure of BOK and its pore-forming activity, we hypothesized that cBID function could be substituted by administration of heat. The incubation of $BOK^{\Delta C}$ and BAX with mildly increased temperatures indeed provided enough energy to induce conformational changes responsible for their insertion in the lipid bilayer. Interestingly, in cells stressed by heat, BAX undergoes conformational changes, translocation to the mitochondria and apoptosis characterized by a significant calcium dyshomeostasis [40]. A thrilling possibility emerging form this stress model is that BOK might be also activated by the treatment, thus compromising the calcium homeostasis in the cell during the cell death.

An intriguing result from our work is that, despite of all the above *in vitro* evidence of $BOK^{\Delta C}$ being able to permeabilize artificial membranes, we did not find evidence for $BOK^{\Delta C}$ -mediated cytochrome c release from enriched mitochondrial fractions derived from *Bax*$^{-/-}$*Bak*$^{-/-}$ MEFs, not even when cBID was added or heat was provided to the reaction mixture. This result contrasts with reports that BOK can trigger the intrinsic apoptotic pathway independently of BAX/BAK [14, 34]. However, neither of those studies provided direct proof of cytochrome c release by recombinant BOK on isolated mitochondria. Our data indicate that the activity of $BOK^{\Delta C}$ in biological membranes might be subjected to important negative regulatory steps or factors overlooked in our assay that deserve further investigation. It remains further possible that, despite its *in vitro* pore-forming potential, $BOK^{\Delta C}$ fails to remodel the mitochondria outer membrane in a way compatible with the release of cytochrome c from the intermembrane space. Additionally, we cannot ignore the possibility that BOK might need its C-terminal tail-anchor for its full activity in mitochondria, despite reports that the C-terminus does not seem to be necessary for BAK [31, 41] or BAX [42, 43] to release cyt. c from isolated mitochondria.

Given that BOK does not dominantly localize to mitochondria and that it does not efficiently release cytochrome c from them when isolated and in the absence of BAX/BAK, we cannot discard the possibility that MOMP-induction may not be the main function of BOK. Considering the nature of the effects when BOK interacts with membranes, it seems conceivable that one main function of BOK could be related with the stabilization of regions of high membrane curvature, which may include non-lamellar structures and membrane pores. Since most BOK is located at the ER, where it has been

shown to interact with IP3R and maybe to play a role in calcium homeostasis, one possibility might be that BOK acts at the ER/mitochondrial contact sites. These sites are responsible for calcium exchange between ER and mitochondria, are enriched in IP3R and likely involve special membrane structures that allow lipid exchange. The presence of BOK at these sites may also allow their regulation by cBID during apoptosis. Although our work sheds light on the molecular mechanism of BOK at the membrane and opens new research possibilities, additional efforts will be required to connect the mechanism of action of BOK with its biological function.

Taken together, we show that $BOK^{\Delta C}$ forms large and stable pores in model membranes, and that $BOK^{\Delta C}$ (and likely full length BOK) activity is cooperatively enhanced by cBID but not blockable by BCL-X_L. However, cytochrome c release from isolated BAX/BAK-deficient mitochondria by $BOK^{\Delta C}$ (with or without cBID) was inefficient compared to BAX/cBID. Although the membrane activity of both proteins in model membranes is very similar, the latter observation clearly distinguishes the properties of $BOK^{\Delta C}$ from those of BAX (and BAK).

EXPERIMENTAL PROCEDURES

Protein expression and purification

pCMV6 containing the full-length mouse *Bok* cDNA (NM_016778.3) was purchased from Origene (SKU: MC206561, Rockville, MD, US). The *Bok* CDS was cloned into the *SapI* restriction sites of the pTXB1 plasmid (New England Biolabs, Ipswich, MA, US), containing the intein-chitin binding domain tag, according to the manufacturer's instructions and sequences confirmed (Microsynth, Balgach, CH). A truncated version of BOK lacking the C-terminal 24 amino acids ($BOK^{\Delta C}$) was created by PCR using the primers 5'-TGCATCACGGGAGATGCA-3' and 5'-GTGGGAGCGGAAGCCAGGA-3'. A five-liter culture of BL21-CodonPlus (DE3)-RIPL *E. coli* strain (Agilent Technologies, Santa Clara, CA, US) harboring the pTXB1-BOKΔC construct was prepared in selective Terrific Broth media (100 µg/mL Ampicillin, 30 µg/mL Chloramphenicol) and protein expression was induced at 20°C for 5h with 1 mM IPTG. The bacterial pellet was collected, resuspended in Chitin Buffer (1 M NaCl, 20 mM Tris-HCl, pH 8.5) supplemented with Complete Protease Inhibitor Cocktail® (Roche Diagnostics AG, Rotkreuz, CH) and disrupted at 11'000 p.s.i in an Emulsiflex-C5 homogenizer (AVESTIN Europe GmbH, Mannheim, DE). The lysate was cleared and recombinant $BOK^{\Delta C}$ captured with chitin-beads (New England Biolabs, GB), followed by DTT-induced intein autolysis during 16h at 4°C. The protein was eluted, dialyzed and further purified by a cation-exchange chromatography using a HiTrap SP FF column (GE Healthcare, GE). Purity, yield, and protein identity were assessed by densitometric analysis of Coomassie stained SDS-PAGE gels using ImageJ [44], protein quantification using the Bradford reagent, western blot (using an in-house rabbit monoclonal anti-BOK antibody, RabMab BOK-1-5 [12]) and mass spectrometry respectively.

Protein purity was >90% (see also Figure 1B, D), except for studies of the influence of the lipid composition BOK membrane activity (Figure 2) where a slightly less pure batch of $BOK^{\Delta C}$ was used. Cleaved cBID (complex of fragments p7 and p15), BAX and BCL-X_L were expressed in *E.coli* and purified as previously described [4, 23, 30].

Preparation of artificial membranes

All the lipids used in this study were purchased from Avanti Polar Lipids (Hamburg, DE), resuspended in chloroform and mixed at the indicated ratios (w/w). LUVs were prepared as described elsewhere [45]. Briefly, each lipid mixture was vacuum dried and resuspended in a solution of 80 mM calcein, pH 7.0 to a final concentration of 4 mg/mL followed by 5 cycles of freeze/thawing in liquid nitrogen. The resulting multilamellar vesicles were extruded 31 times through a 400 µm polycarbonate membrane using a LiposoFast manual emulsifier (AVESTIN Europe GmbH, Mannheim, DE). The non-encapsulated calcein was removed from the mixture using a Sephadex-G50 column previously equilibrated with DPBS from Sigma. Special lipid mixtures modelling the composition of the mitochondrial membrane (MITOmix; PS:CL:PI:PC:PE, 10:8:11:46:25) [23] or the endoplasmic reticulum (ERmix; Sph:PS:PI:PC:PE, 4:4:10:57:25) [46] were prepared according to the reported composition. GUVs were prepared as previously described [33]. Shortly, 5 µL of a 1 mg/mL lipid-chloroform solution containing the dye DiI (<0.05%; Thermofisher) was layered in two platinum electrodes, air dried and immersed in a Teflon chamber containing 300 mM sucrose. The electrodes were wired to a function generator power source and the GUVs were electro-formed by sequential application of 10 Hz, for 2 h and 2 Hz for 30 min.

Calcein release assay

Calcein-loaded LUVs were incubated with serial dilutions of the recombinant proteins or BH3 peptides corresponding to BIM or BID proteins in a fluorescent-compatible 96-well microtiter plate (NUNC). Calcein release was monitored by fluorescence emission at 520 nm ($\lambda_{excitation}$= 495 nm) during two hours in an Infinite M200 plate reader (Tecan, Mainz, DE). The percentage dye release was calculated as follows:

$Calcein_{release}\,(\%\,of\,\max) = 100 * \frac{(F^{Sample} - F^{Buffer})}{(F^{TX100} - F^{Buffer})}$, were all the terms refer to the maximum fluorescence registered in the wells incubated with the studied proteins (F^{Sample}), with 0.125% Triton-X100 (F^{TX100}) or DPBS (F^{Buffer}). The maximum values were obtained by curve fitting to a hyperbole or, in those cases where calcein self-quenched due to a massive release, it was assigned to the maximum value before the quenching started. The effective concentration of $BOK^{\Delta C}$ was corrected

between batches according to the individual EC_{50} values. The sequences for the BH3 peptides are the following: BID-BH3(IARHLAQVGDSMD), BIM-BH3(IAQELRRIGDEFN).

GUVs permeabilisation experiments

GUVs permeabilisation assays were performed according to [23]. Briefly, 70 µL of GUVs made from MITOmix were incubated at 25°C for 1 h in a casein-coated LabTec chamber (NUNC) containing cyt. c_{488}, APC and the studied proteins dissolved in DPBS. The total volume in each reaction chamber is 300 µL. After the incubation time at least five pictures of each condition were taken using a LSM710 microscope with a C-Apochromat 40 1.2 water immersion objective (Zeiss, Oberkochen, DE). A similar setup was prepared for the heat activation of $BOK^{\Delta C}$ in GUVs, just setting the reaction temperature to 42°C for 45 min, before allowing the samples to cool down to RT before the pictures were taken. The evaluation of the pore stability was adapted from Bleicken *et al*. [30]. Shortly, GUVs were incubated for 45 min at RT with or without the indicated BCL-2 proteins in DPBS containing AF555 as an indicator of the permeabilisation status of the vesicles. Afterwards, cyt. c_{488} and APC were added to the mixture and the pictures were taken 15 min later. For each experiment, the GUVs permeabilisation degree to the analyzed dyes was determined using the GUVs detector software available at http://www.ifib.uni-tuebingen.de/research/garcia-saez/GUVs-software.html [47]. The threshold for considering a GUV permeated was arbitrarily set at 30% with the exception of the pore stability assays where it was set up to 50 %, 35% and 40% for AF555, cyt. c_{488} and APC respectively. Data was analyzed using R version 3.2.1 [48] and visualized using the *ggplot2* package [49].

Mitochondria isolation

Cell cultures in exponential growth phase of *Bax*$^{-/-}$*Bak*$^{-/-}$ SV40 large T antigen immortalized mouse embryo fibroblasts (SV40 MEF) were trypsinized, washed with DPBS and incubated for 15 minutes in MB buffer (210 mM mannitol, 70 mM sucrose, 1 mM EDTA, 10 mM HEPES pH 7,5 supplemented with Complete Protease Inhibitor Cocktail (Roche, CH). The cells were manually disrupted by 18 passages through a 27 G needle, and the debris was removed by centrifugation at 2'500 x g (3 x 5 min). The mitochondria-enriched fraction was obtained by centrifugation for 10 min at 10' 000 x g, resuspended in MB-EGTA buffer (MB buffer with 1 mM EGTA instead of EDTA) and its protein concentration determined by Bradford assay (Biorad, Cressier, CH). The mitochondrial preparations were immediately used for the cytochrome c release assays.

Cytochrome c release assays

Cytochrome c release from mitochondria was performed as previously reported [50]. Briefly, 30 µg of mitochondria were incubated with the following protein amounts unless indicated otherwise (100 nM $BOK^{\Delta C}$, 50nM cBID, 100 nM BAX) in KCL buffer (125 mM KCl, 4 mM $MgCl_2$, 5 mM KH_2PO_4, 10 mM HEPES pH 7,4, 0,5 mM EGTA) for 60 min at 37 °C. The supernatant was collected and the pellet was washed with KCl buffer, followed by addition of Laemmli buffer. For the experiments using heat-activated $BOK^{\Delta C}$, we proceeded as described by [31] with minor modifications. Shortly, the recombinant proteins were heated at 43°C for 1 h in the presence of the isolated mitochondria in KCL buffer. Pellet and supernatant were separated afterwards by centrifugation. The presence of cyt. c in the fractions was determined by western blotting using a mouse monoclonal anti-cyt. c antibody (BD Biosciences, clone 7H8.2C12).

Membrane binding assays.

Crude mitochondria preparations from *Bok*$^{-/-}$ SV40 MEF were incubated with the indicated combinations of recombinant proteins (200 nM $BOK^{\Delta C}$, 100nM cBID) at 37°C for 1 h. Afterwards the samples were fractionated by centrifugation or linear sucrose gradient (1-2M). The samples processed by sucrose gradient were ultracentrifuged at 50'000 x g in a swinging bucket SW41 rotor (Beckman Coulter, Nyon, CH) during 90 min. The gradients were then split in 1 mL fractions and precipitated using methanol/ chloroform. The distribution of the recombinant proteins across the gradient was detected by western blotting using the corresponding antibodies: rabbit monoclonal anti BOK (RabMab BOK-1-5 [12]), rabbit polyclonal anti-BAX (Santa Cruz Biotechnology, sc-493), mouse monoclonal anti-porin (Calbiochem, clone 89-173/016).

ACKNOWLEDGMENTS

We thank Caroline Stegmueller for the exceptional technical support and Dr. Christoph Borner (Freiburg, DE) for *Bax*$^{-/-}$*Bak*$^{-/-}$ MEF. This work was supported by the Swiss National Science Foundation (SNF), Grant 310030E150805, part of the D-A-CH initiative from the SNF and the Deutsche Forschungsgemeinschaft (DFG), FOR-2036 (to T.K.) and the DFG GA1641/2-1 (to A.J.G.S.). Y.F.M. is a PhD student of the Graduate School of Cellular and Biomedical Sciences of the University of Bern. S.B. and A.J.G.S. were additionally supported by European Research Council (ERC-2012-StG-309966) and S.B. by the Cluster of Excellence RESOLV (EXC 1069) funded by the DFG.

AUTHOR CONTRIBUTIONS

YFM performed most of the experiments, analyzed data and wrote the manuscript. **SB** planed and performed experiments, analyzed data and wrote the manuscript. **KKD** and **DB** performed experiments and analyzed data. **AJGS** and **TK** designed the study, planned the experiments and wrote the manuscript.

REFERENCES

1. Youle, R. J. & Strasser, A. (2008) The BCL-2 protein family: opposing activities that mediate cell death, *Nat Rev Mol Cell Biol.* **9**, 47-59.
2. Newmeyer, D. D. & Ferguson-Miller, S. (2003) Mitochondria: releasing power for life and unleashing the machineries of death, *Cell.* **112**, 481-90.
3. Willis, S. N., Chen, L., Dewson, G., Wei, A., Naik, E., Fletcher, J. I., Adams, J. M. & Huang, D. C. (2005) Proapoptotic Bak is sequestered by Mcl-1 and Bcl-xL, but not Bcl-2, until displaced by BH3-only proteins, *Genes Dev.* **19**, 1294-305.
4. Bleicken, S., Classen, M., Padmavathi, P. V., Ishikawa, T., Zeth, K., Steinhoff, H. J. & Bordignon, E. (2010) Molecular details of Bax activation, oligomerization, and membrane insertion, *J Biol Chem.* **285**, 6636-47.
5. Chipuk, J. E., McStay, G. P., Bharti, A., Kuwana, T., Clarke, C. J., Siskind, L. J., Obeid, L. M. & Green, D. R. (2012) Sphingolipid metabolism cooperates with BAK and BAX to promote the mitochondrial pathway of apoptosis, *Cell.* **148**, 988-1000.
6. Raemy, E. & Martinou, J. C. (2014) Involvement of cardiolipin in tBID-induced activation of BAX during apoptosis, *Chem Phys Lipids.* **179**, 70-4.
7. Lucken-Ardjomande, S., Montessuit, S. & Martinou, J. C. (2008) Contributions to Bax insertion and oligomerization of lipids of the mitochondrial outer membrane, *Cell Death Differ.* **15**, 929-37.
8. Kuwana, T., Mackey, M. R., Perkins, G., Ellisman, M. H., Latterich, M., Schneiter, R., Green, D. R. & Newmeyer, D. D. (2002) Bid, Bax, and lipids cooperate to form supramolecular openings in the outer mitochondrial membrane, *Cell.* **111**, 331-42.
9. Shamas-Din, A., Bindner, S., Chi, X., Leber, B., Andrews, D. W. & Fradin, C. (2015) Distinct lipid effects on tBid and Bim activation of membrane permeabilization by pro-apoptotic Bax, *Biochem J.* **467**, 495-505.
10. Raemy, E., Montessuit, S., Pierredon, S., van Kampen, A. H., Vaz, F. M. & Martinou, J. C. (2016) Cardiolipin or MTCH2 can serve as tBID receptors during apoptosis, *Cell Death Differ.* **23**, 1165-74.
11. Hsu, S. Y., Kaipia, A., McGee, E., Lomeli, M. & Hsueh, A. J. (1997) Bok is a pro-apoptotic Bcl-2 protein with restricted expression in reproductive tissues and heterodimerizes with selective anti-apoptotic Bcl-2 family members, *Proc Natl Acad Sci U S A.* **94**, 12401-6.
12. Echeverry, N., Bachmann, D., Ke, F., Strasser, A., Simon, H. U. & Kaufmann, T. (2013) Intracellular localization of the BCL-2 family member BOK and functional implications, *Cell Death Differ.* **20**, 785-99.
13. Ke, F., Voss, A., Kerr, J. B., O'Reilly, L. A., Tai, L., Echeverry, N., Bouillet, P., Strasser, A. & Kaufmann, T. (2012) BCL-2 family member BOK is widely expressed but its loss has only minimal impact in mice, *Cell Death Differ.* **19**, 915-25.
14. Llambi, F., Wang, Y. M., Victor, B., Yang, M., Schneider, D. M., Gingras, S., Parsons, M. J., Zheng, J. H., Brown, S. A., Pelletier, S., Moldoveanu, T., Chen, T. & Green, D. R. (2016) BOK Is a Non-canonical BCL-2 Family Effector of Apoptosis Regulated by ER-Associated Degradation, *Cell.* **165**, 421-33.
15. Elsayed, M. M. & Cevc, G. (2011) The vesicle-to-micelle transformation of phospholipid-cholate mixed aggregates: a state of the art analysis including membrane curvature effects, *Biochim Biophys Acta.* **1808**, 140-53.

16. Ke, F., Bouillet, P., Kaufmann, T., Strasser, A., Kerr, J. & Voss, A. K. (2013) Consequences of the combined loss of BOK and BAK or BOK and BAX, *Cell Death Dis.* **4**, e650.
17. Ke, F., Grabow, S., Kelly, G. L., Lin, A., O'Reilly, L. A. & Strasser, A. (2015) Impact of the combined loss of BOK, BAX and BAK on the hematopoietic system is slightly more severe than compound loss of BAX and BAK, *Cell Death Dis.* **6**, e1938.
18. Ray, J. E., Garcia, J., Jurisicova, A. & Caniggia, I. (2010) Mtd/Bok takes a swing: proapoptotic Mtd/Bok regulates trophoblast cell proliferation during human placental development and in preeclampsia, *Cell Death Differ.* **17**, 846-59.
19. D'Orsi, B., Engel, T., Pfeiffer, S., Nandi, S., Kaufmann, T., Henshall, D. C. & Prehn, J. H. (2016) Bok Is Not Pro-Apoptotic But Suppresses Poly ADP-Ribose Polymerase-Dependent Cell Death Pathways and Protects against Excitotoxic and Seizure-Induced Neuronal Injury, *J Neurosci.* **36**, 4564-78.
20. Schulman, J. J., Wright, F. A., Kaufmann, T. & Wojcikiewicz, R. J. (2013) The Bcl-2 protein family member Bok binds to the coupling domain of inositol 1,4,5-trisphosphate receptors and protects them from proteolytic cleavage, *J Biol Chem.* **288**, 25340-9.
21. Schulman, J. J., Wright, F. A., Han, X., Zluhan, E. J., Szczesniak, L. M. & Wojcikiewicz, R. J. (2016) The Stability and Expression Level of Bok Are Governed by Binding to Inositol 1,4,5-Trisphosphate Receptors, *J Biol Chem.* **291**, 11820-8.
22. Suzuki, M., Youle, R. J. & Tjandra, N. (2000) Structure of Bax: coregulation of dimer formation and intracellular localization, *Cell.* **103**, 645-54.
23. Bleicken, S., Wagner, C. & Garcia-Saez, A. J. (2013) Mechanistic differences in the membrane activity of Bax and Bcl-xL correlate with their opposing roles in apoptosis, *Biophys J.* **104**, 421-31.
24. Champion, K. M., Nishihara, J. C., Joly, J. C. & Arnott, D. (2001) Similarity of the Escherichia coli proteome upon completion of different biopharmaceutical fermentation processes, *Proteomics.* **1**, 1133-48.
25. Wu, S., Wan, P., Li, J., Li, D., Zhu, Y. & He, F. (2006) Multi-modality of pI distribution in whole proteome, *Proteomics.* **6**, 449-55.
26. Adhikari, S., Manthena, P. V., Sajwan, K., Kota, K. K. & Roy, R. (2010) A unified method for purification of basic proteins, *Anal Biochem.* **400**, 203-6.
27. Fosnaric, M., Bohinc, K., Gauger, D. R., Iglic, A., Kralj-Iglic, V. & May, S. (2005) The influence of anisotropic membrane inclusions on curvature elastic properties of lipid membranes, *J Chem Inf Model.* **45**, 1652-61.
28. Terrones, O., Antonsson, B., Yamaguchi, H., Wang, H. G., Liu, J., Lee, R. M., Herrmann, A. & Basanez, G. (2004) Lipidic pore formation by the concerted action of proapoptotic BAX and tBID, *J Biol Chem.* **279**, 30081-91.
29. Bleicken, S., Hofhaus, G., Ugarte-Uribe, B., Schroder, R. & Garcia-Saez, A. J. (2016) cBid, Bax and Bcl-xL exhibit opposite membrane remodeling activities, *Cell Death Dis.* **7**, e2121.
30. Bleicken, S., Landeta, O., Landajuela, A., Basanez, G. & Garcia-Saez, A. J. (2013) Proapoptotic Bax and Bak proteins form stable protein-permeable pores of tunable size, *J Biol Chem.* **288**, 33241-52.
31. Pagliari, L. J., Kuwana, T., Bonzon, C., Newmeyer, D. D., Tu, S., Beere, H. M. & Green, D. R. (2005) The multidomain proapoptotic molecules Bax and Bak are directly activated by heat, *Proc Natl Acad Sci U S A.* **102**, 17975-80.
32. Subburaj, Y., Cosentino, K., Axmann, M., Pedrueza-Villalmanzo, E., Hermann, E., Bleicken, S., Spatz, J. & Garcia-Saez, A. J. (2015) Bax monomers form dimer units in the membrane that further self-assemble into multiple oligomeric species, *Nat Commun.* **6**, 8042.
33. Bleicken, S. & Garcia-Saez, A. J. (2014) New biophysical methods to study the membrane activity of Bcl-2 proteins, *Methods Mol Biol.* **1176**, 191-207.
34. Einsele-Scholz, S., Malmsheimer, S., Bertram, K., Stehle, D., Johanning, J., Manz, M., Daniel, P. T., Gillissen, B. F., Schulze-Osthoff, K. & Essmann, F. (2016) Bok is a genuine multi-BH-domain protein that triggers apoptosis in the absence of Bax and Bak, *J Cell Sci.* **129**, 2213-23.
35. Carpio, M. A., Michaud, M., Zhou, W., Fisher, J. K., Walensky, L. D. & Katz, S. G. (2015) BCL-2 family member BOK promotes apoptosis in response to endoplasmic reticulum stress, *Proc Natl Acad Sci U S A.* **112**, 7201-6.

36. Fernandez-Marrero, Y., Ke, F., Echeverry, N., Bouillet, P., Bachmann, D., Strasser, A. & Kaufmann, T. (2016) Is BOK required for apoptosis induced by endoplasmic reticulum stress?, *Proc Natl Acad Sci U S A.* **113**, E492-3.
37. McMahon, H. T. & Boucrot, E. (2015) Membrane curvature at a glance, *J Cell Sci.* **128**, 1065-70.
38. Salvador-Gallego, R., Mund, M., Cosentino, K., Schneider, J., Unsay, J., Schraermeyer, U., Engelhardt, J., Ries, J. & Garcia-Saez, A. J. (2016) Bax assembly into rings and arcs in apoptotic mitochondria is linked to membrane pores, *EMBO J.* **35**, 389-401.
39. Hsu, S. Y. & Hsueh, A. J. (1998) A splicing variant of the Bcl-2 member Bok with a truncated BH3 domain induces apoptosis but does not dimerize with antiapoptotic Bcl-2 proteins in vitro, *J Biol Chem.* **273**, 30139-46.
40. Gu, Z. T., Li, L., Wu, F., Zhao, P., Yang, H., Liu, Y. S., Geng, Y., Zhao, M. & Su, L. (2015) Heat stress induced apoptosis is triggered by transcription-independent p53, Ca(2+) dyshomeostasis and the subsequent Bax mitochondrial translocation, *Sci Rep.* **5**, 11497.
41. Landeta, O., Landajuela, A., Gil, D., Taneva, S., Di Primo, C., Sot, B., Valle, M., Frolov, V. A. & Basanez, G. (2011) Reconstitution of proapoptotic BAK function in liposomes reveals a dual role for mitochondrial lipids in the BAK-driven membrane permeabilization process, *J Biol Chem.* **286**, 8213-30.
42. Priault, M., Cartron, P. F., Camougrand, N., Antonsson, B., Vallette, F. M. & Manon, S. (2003) Investigation of the role of the C-terminus of Bax and of tc-Bid on Bax interaction with yeast mitochondria, *Cell Death Differ.* **10**, 1068-77.
43. Wieckowski, M. R., Vyssokikh, M., Dymkowska, D., Antonsson, B., Brdiczka, D. & Wojtczak, L. (2001) Oligomeric C-terminal truncated Bax preferentially releases cytochrome c but not adenylate kinase from mitochondria, outer membrane vesicles and proteoliposomes, *FEBS Lett.* **505**, 453-9.
44. Schneider, C. A., Rasband, W. S. & Eliceiri, K. W. (2012) NIH Image to ImageJ: 25 years of image analysis, *Nat Methods.* **9**, 671-5.
45. Garcia-Saez, A. J., Coraiola, M., Serra, M. D., Mingarro, I., Muller, P. & Salgado, J. (2006) Peptides corresponding to helices 5 and 6 of Bax can independently form large lipid pores, *FEBS J.* **273**, 971-81.
46. Davison, S. C. & Wills, E. D. (1974) Studies on the lipid composition of the rat liver endoplasmic reticulum after induction with phenobarbitone and 20-methylcholanthrene, *Biochem J.* **140**, 461-8.
47. Hermann, E., Bleicken, S., Subburaj, Y. & Garcia-Saez, A. J. (2014) Automated analysis of giant unilamellar vesicles using circular Hough transformation, *Bioinformatics.* **30**, 1747-54.
48. Team, R. C. (2015) R: A Language and Environment for Statistical Computing, R Foundation for Statistical Computing.
49. Wickham, H. (2009) *ggplot2 : elegant graphics for data analysis*, Springer, New York.
50. Wilfling, F., Weber, A., Potthoff, S., Vogtle, F. N., Meisinger, C., Paschen, S. A. & Hacker, G. (2012) BH3-only proteins are tail-anchored in the outer mitochondrial membrane and can initiate the activation of Bax, *Cell Death Differ.* **19**, 1328-36.

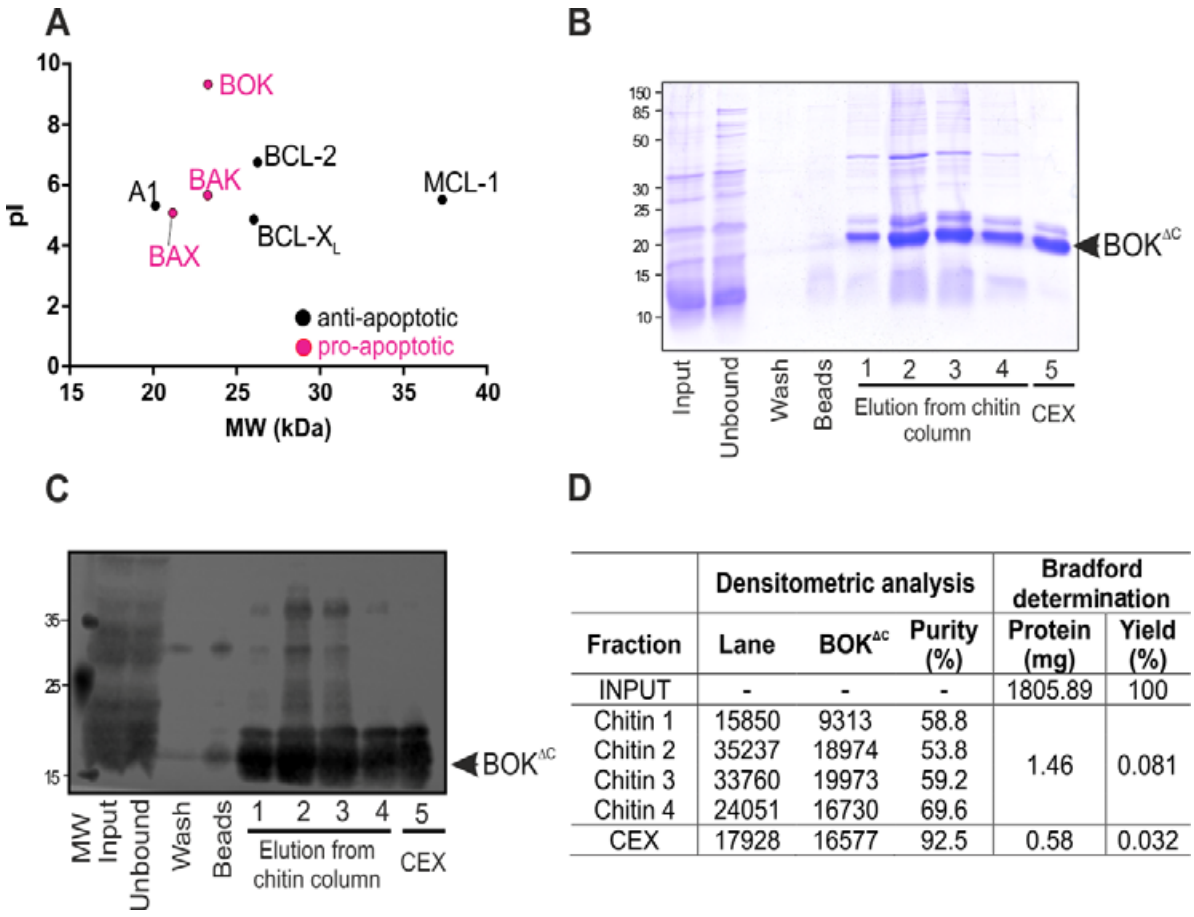

	Densitometric analysis			Bradford determination	
Fraction	Lane	BOK$^{\Delta C}$	Purity (%)	Protein (mg)	Yield (%)
INPUT	-	-	-	1805.89	100
Chitin 1	15850	9313	58.8	1.46	0.081
Chitin 2	35237	18974	53.8		
Chitin 3	33760	19973	59.2		
Chitin 4	24051	16730	69.6		
CEX	17928	16577	92.5	0.58	0.032

FIGURE 1. Purification of recombinant BOK$^{\Delta C}$ using a two-step affinity-based strategy. (A) Predicted isoelectric point of multidomain BCL-2 family members (based on Expasy Compute pI/Mw tool, http://web.expasy.org/compute_pi/). (B) Representative coomassie stained SDS-PAGE gel evaluating the purification process of recombinant BOK. ***Beads***: 10 µL of chitin beads after lysate input and before DTT-induced intein cleavage, **CEX**: cation affinity chromatography. (C) Inmunoblot of the same samples from panel B using a rabbit monoclonal anti-BOK antibody. (D) Purification tables for a typical production of recombinant BOK$^{\Delta C}$.

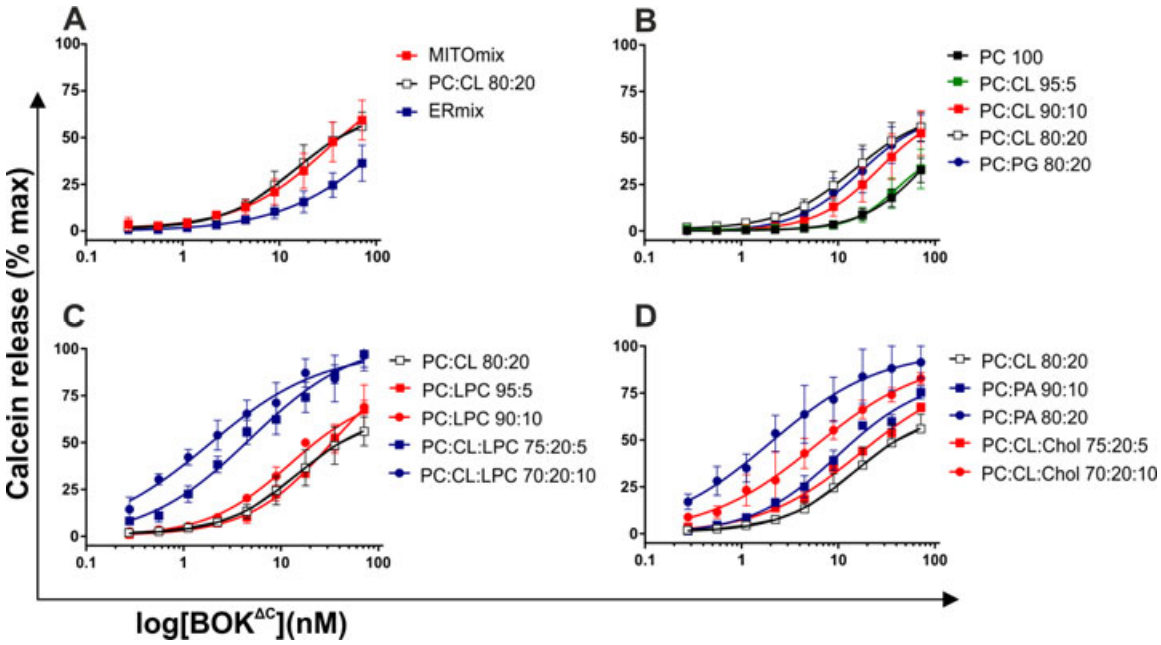

FIGURE 2. The lipid composition modulates the permeabilisation potential of BOK$^{\Delta C}$. Several lipid mixtures were used to determine the influence on BOK$^{\Delta C}$ -mediated permeabilisation of: (A) vesicles mimicking mitochondria (MITOmix) or endoplasmic reticulum (ERmix), (B) negatively charged lipids (CL), (C) positive curvature inducers (LPC) and (D) non-lamellar compatible lipids (PA) together with a neutral negative curvature inducer lipid (Chol). Lipid ratios are indicated for each composition as molar percentages. Calcein release was normalized to the maximum release induced by Triton-X100 on each sample. **PC**:phosphatidylcholine, **CL**: cardiolipin, **PG**: phosphatidylglycerol, **LPC**: lyso-phosphatidylcholine, **PA**:phosphatidic acid, **Chol**: cholesterol. Values correspond to mean ± SEM; N=3.

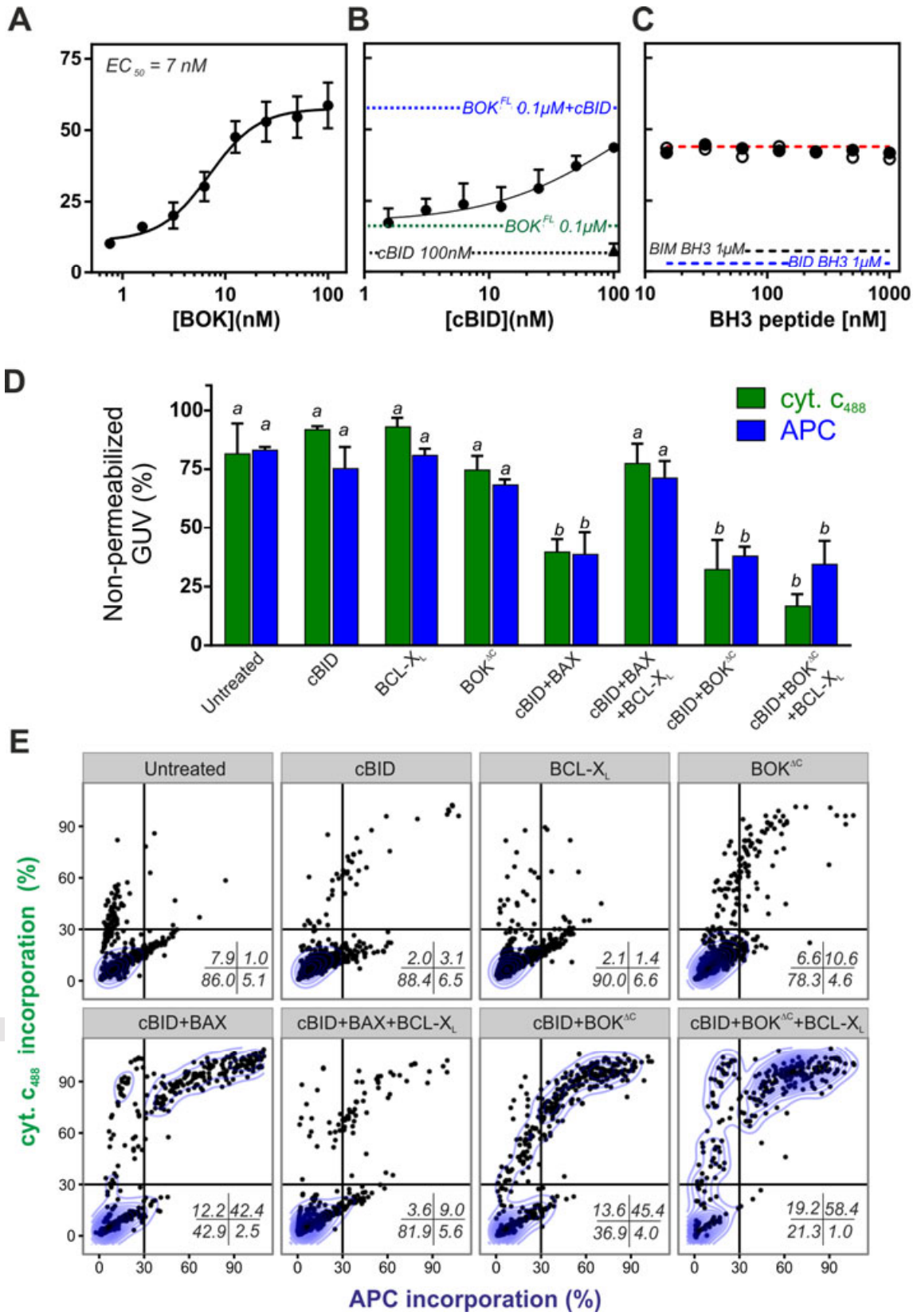

FIGURE 3. BOK$^{\Delta C}$ -mediated vesicle permeabilisation is enhanced by cBID and allows the passage of molecules of up to 104 kDa. (A) Determination of EC_{50} value for BOK$^{\Delta C}$ in PC:CL 80:20 vesicles. (B) Calcein release from PC:CL 80:20 liposomes-using BOK$^{\Delta C}$ at the EC_{50} concentration and variable amounts of cBID or (C) increasing concentration of BH3 peptides. Dashed lines represents

the maximum calcein release promoted by 100 nM cBID, 0.1 µM full length BOK ± 50 nM cBID or 1 µM of the indicated BH3 peptides. (D) Fraction of non-permeabilized GUV to cyt. c_{488} (12 kDa) or APC (104 kDa) 60 min after treatment with different combinations of cBID (10 nM), $BOK^{\Delta C}$ (10 nM), BCL-X_L (50 nM) and BAX (20 nM). Bars correspond to mean ± SEM; N=3. (E) Percentage of filling degree to the indicated fluorescent proteins for each individual vesicle across the indicated treatments. The percentage of GUV on each quadrant is indicated. Statistical differences were calculated with a two-way ANOVA correcting the *p*-values using the Benjamini-Krieger-Yekutieli method. Shared letters indicate non-significant differences with *p*-values of at least 0.05.

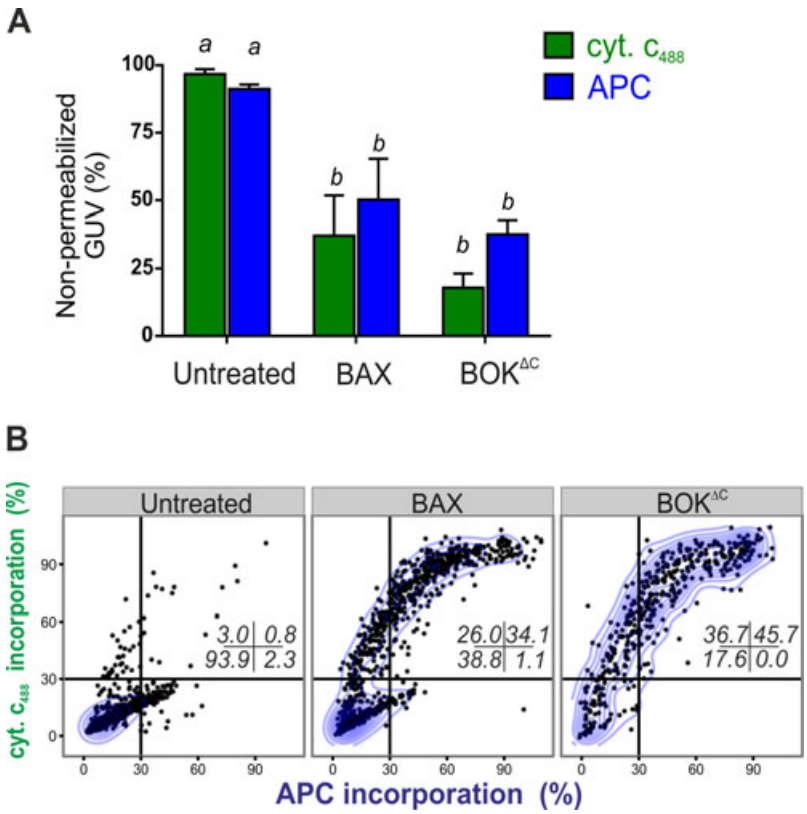

FIGURE 4. $BOK^{\Delta C}$ can be activated by temperature. (A) Percentage of non-permeabilized MITOmix-derived GUVs to cyt. c_{488} and APC after incubation at 42°C for 45 min with 20 nM BAX or 10 nM BOK. Bars correspond to mean ± SEM; N=3. (B) Percentage of filling degree to the indicated fluorescent proteins for each individual vesicle across the treatments. The percentage of GUV on each quadrant is indicated. Statistical differences were calculated with a two-way ANOVA correcting the *p*-values using the Benjamini-Krieger-Yekutieli method. Shared letters indicate non-significant differences with *p*-values of at least 0.05.

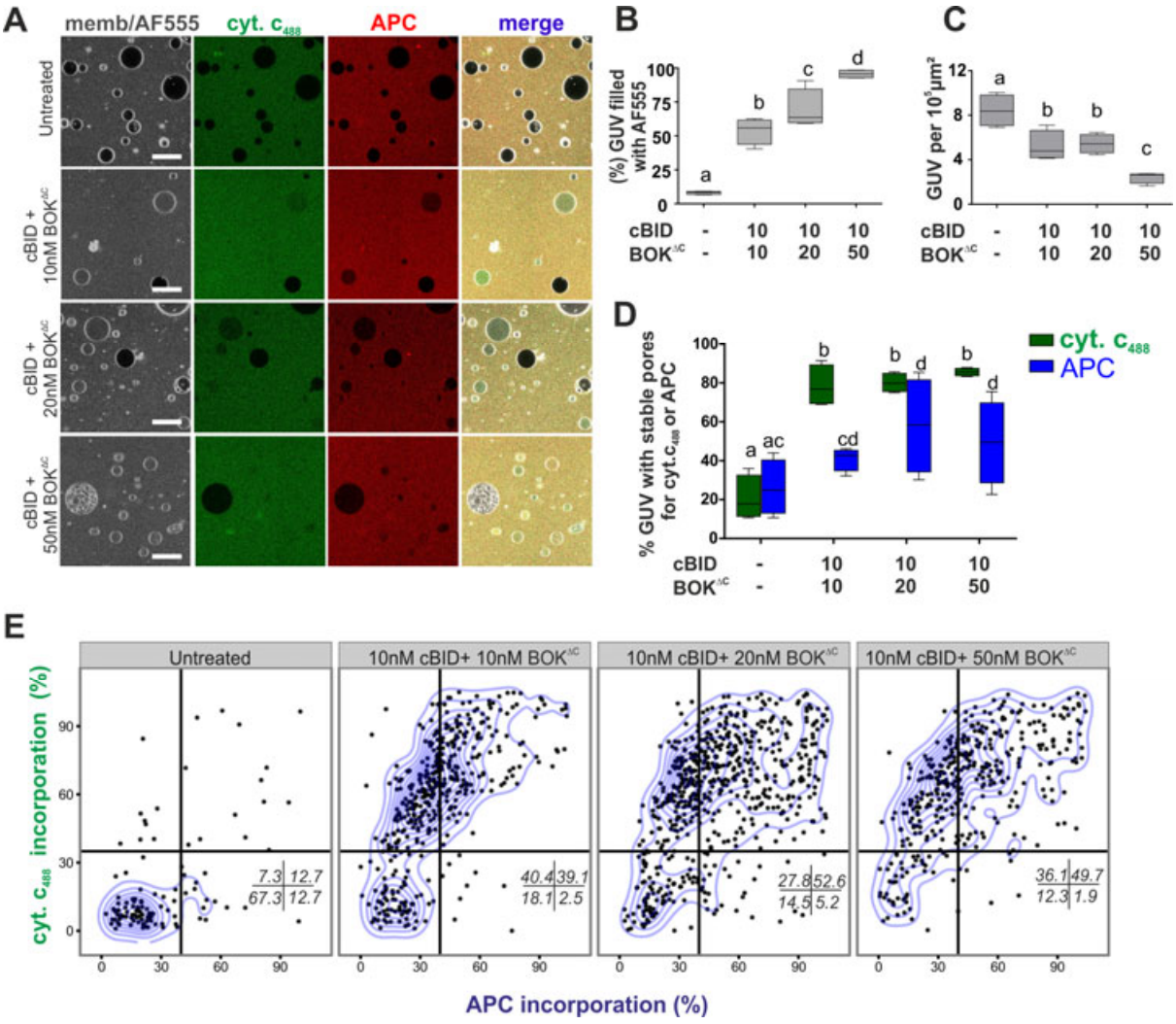

FIGURE 5. Pores formed by BOK$^{\Delta C}$ are stable over time. (A) Representative pictures for the MITOmix-made GUV incubated during 45 min with the indicated proteins in the presence of AF555, followed by addition of cyt. c_{488} and APC. Bars represent 50 µm. (B) Determination of the AF555 degree of incorporation into the GUV using a filling threshold of 50%. (C) Number of GUV *per* area across the treatments. (D) Filling degree to cyt. c_{488} and APC in those GUVs already filled with AF555 (>50%). (E) Percentage of filling degree to the indicated fluorescent proteins on each individual vesicle across the samples. Whiskers cover 10th-90th percentile; N=4. Statistical differences were calculated with a one-way (B, C) or two-way ANOVA correcting the *p*-values using the Benjamini-Krieger-Yekutieli method. Shared letters indicate non-significant differences with *p*-values of at least 0.05.

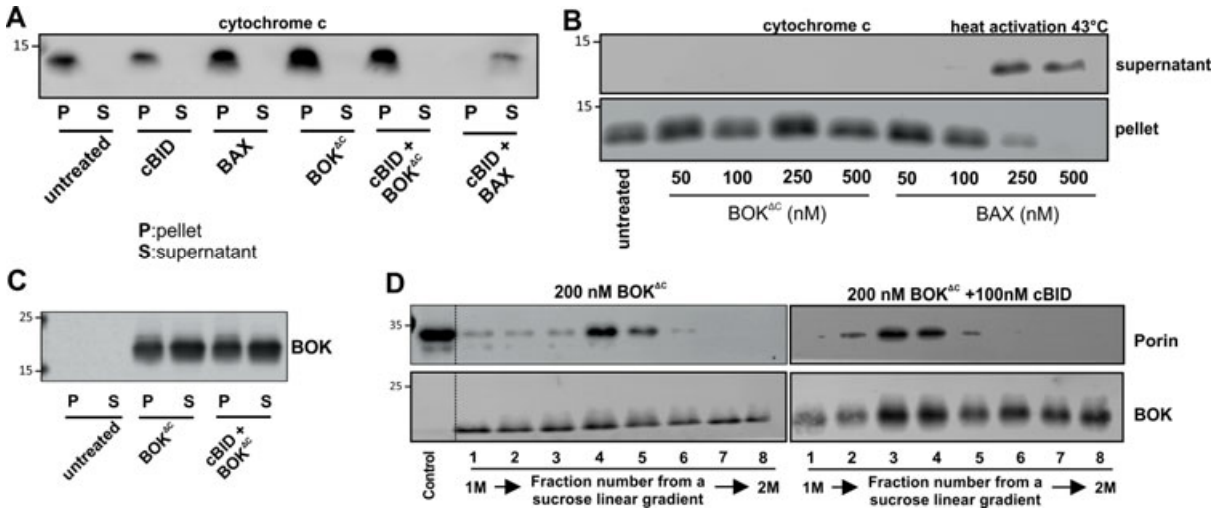

FIGURE 6. Binding of BOK$^{\Delta C}$ to isolated BAX/BAK-deficient mitochondria is not sufficient for cytochrome c release. Mitochondria isolated from *Bax*$^{-/-}$*Bak*$^{-/-}$ (A, B) or *Bok*$^{-/-}$ (C, D) SV40 MEF were incubated during 1 h at 37°C (A, C, D) or 43°C (B) with combinations of 50 nM cBID, 100 nM BOK$^{\Delta C}$ or 100 nM BAX; unless indicated otherwise. The release of cytochrome c (A, B) was assessed immediately after the assay by immunoblotting of pellet (mitochondria) and supernatant fractions, respectively. (C) BOK$^{\Delta C}$ interacts with membranes in mitochondrial preparation independent of the presence of cBID. (D) BOK$^{\Delta C}$ interacts with intracellular membranes not restricted to mitochondria and irrespective of the presence of cBID. Presented data is representative of at least 3 independent experiments.